# Tanshinone IIA attenuates experimental autoimmune encephalomyelitis in rats

JUN YAN, XUE YANG, DONG HAN and JUAN FENG

Department of Neurology, The Shengjing Hospital of China Medical University, Shenyang, Liaoning 110004, P.R. China

Received July 27, 2015; Accepted May 26, 2016

DOI: 10.3892/mmr.2016.5431

**Abstract.** Multiple sclerosis (MS) is an inflammatory autoimmune neurodegenerative disease, which features focal demyelination and inflammatory cell infiltration of the brain and the spinal cord. Tanshinone IIA (TSIIA), one of the major fat-soluble components of *Salvia miltiorrhiza* (Danshen), has anti-inflammatory, immunoregulatory and neuroprotective activity; however, its efficacy in MS remains unknown. The current study was designed to investigate the potential therapeutic function of TSIIA on MS in the experimental autoimmune encephalomyelitis (EAE) rat model. In comparison to the vehicle control group, the TSIIA-treated groups showed notably improved clinical symptoms and pathological changes, including central nervous system inflammatory cell infiltration and demyelination. Following administration of TSIIA, the quantity of $CD4^+$ T cells, $CD8^+$ T cells and macrophages/microglia in the spinal cord were reduced to different extents. Furthermore, TSIIA was also shown to downregulate interleukin (IL)-17 and IL-23 levels in the brain and serum of EAE rats. The results collectively provide evidence that TSIIA alleviates EAE and support its utility as a novel therapy for MS.

## Introduction

MS is a progressive autoimmune demyelinating disorder of the central nervous system (CNS), which is mediated via various inflammatory cells and cytokines. Experimental autoimmune encephalomyelitis (EAE) has been universally acknowledged as an animal model for MS, as it has similar clinical and neuropathological features (1). In MS/EAE, once activated, circulating T cells travel from the periphery to the CNS and generate large amounts of proinflammatory cytokines. Then microglia and invaded macrophages are consequently activated, and stimulate autoimmune reactions, leading to myelin damage. $CD4^+$ T cells are the predominant cell type involved in the pathology of MS/EAE. Mice without functional $CD4^+$ T cells do not develop the relevant clinical signs of disease (2). $CD8^+$ T cells also accumulate and activate microglia to an extent, causing tissue damage during CNS autoimmunity (3). In the CNS, Mac-1 is expressed predominantly on the surface of resident microglia cells and infiltrating inflammatory macrophages, and therefore used to identify activated microglia/macrophages in EAE (4).

The interleukin (IL)-23/IL-17 axis performs important functions in MS pathogenesis. IL-23 is predominantly secreted from activated macrophages/microglia and dendritic cells (5), inducing Th0 cell differentiation into Th17 cells (6). This type of shift facilitates CNS inflammation and the development of EAE. Th17 cells are characterized by the secretion of IL-17. IL-23 and IL-17 in the serum and CNS have been reported to serve an important role in the pathology and immunotherapy of MS (7).

MS is a debilitating disease with high disability and recurrence rates and there are over one million people worldwide suffering from the disease (8). The treatment of MS is limited to chemically synthesized immunomodulatory or immunosuppressive reagents, which are not always effective and are often associated with severe side-effects (9). Thus, the identification of more effective and safe agents is urgently required. *Salvia miltiorrhiza*, a Chinese herbal medicine, has traditionally been used to treat cardiovascular and cerebrovascular diseases (10,11). Tanshinone IIA (TSIIA), its major bioactive constituent, has been shown to exert immunomodulatory effects on various immune cells and cytokines, with anti-inflammatory, anti-oxidative and neuroprotective functions (12). TSIIA has been shown to exert a therapeutic effect in neurodegenerative diseases, such as Parkinson's (13) and Alzheimer's disease (14). It has also been shown to be effective in inflammatory and autoimmunity diseases, including acute lung inflammation (15), sepsis (16) and systemic sclerosis (17).

Considering these findings, the present study examined the hypothesis that TSIIA can be effectively used for EAE treatment. To the best of our knowledge, this is the first study to demonstrate that TSIIA alleviates EAE by downregulating the IL-23/IL-17 inflammatory pathway and reducing the infiltration of immune cell populations supporting its potential as an effective therapeutic agent for MS.

*Correspondence to:* Dr Juan Feng, Department of Neurology, The Shengjing Hospital of China Medical University, 36 Sanhao Street, Shenyang, Liaoning 110004, P.R. China
E-mail: fengjuanneurology@yahoo.com

*Key words:* tanshinone IIA, interleukin-23, interleukin-17, experimental autoimmune encephalomyelitis

## Materials and methods

*Reagents and animals*. *Mycobacterium tuberculosis* H37Ra was purchased from Difco Laboratories, Inc. (Detroit, MI, USA). TSIIA was obtained from Xi'an Guan Sheng Yuan Co. Ltd. (Xi'an, China). Complete Freund's adjuvant (CFA), Luxol Fast Blue (LFB) and protease inhibitors were purchased from Sigma-Aldrich (St. Louis, MO, USA). Rat IL-17 (SEA063Ra) and rat IL-23 (SEA384Ra) enzyme-linked immunosorbent assay (ELISA) kits were obtained from Cloud-Clone Corp. (Wuhan, China). Mouse anti-β-actin monoclonal antibody (sc-130300), rabbit anti-CD4 polyclonal antibody (sc-7219), rabbit anti-CD8 (sc-7188) polyclonal antibody, peroxidase-conjugated goat anti-rabbit secondary antibody, luminol reagent and radioimmunoprecipitation assay (RIPA) buffer were purchased from Santa Cruz Biotechnology Inc. (Dallas, TX, USA). Rabbit anti-Mac-1 polyclonal antibody (DF6476) and rabbit anti-IL-17 polyclonal antibody (DF6127) were obtained from Affinity Biosciences (Cincinnati, OH, USA). Rabbit anti-IL-23 polyclonal antibody (bs-18146R) was purchased from Beijing Bioss Biological Technology Co., Ltd. (Beijing, China). Biotin-labeled anti-rabbit IgG (SP KIT-C3) was purchased from Beijing Dingguo Changsheng Biotechnology Co., Ltd. (Beijing, China). The goat anti-mouse secondary antibody (SA00001-1) and peroxidase-conjugated goat anti-rabbit secondary antibody (SA00001-2) were purchased from Proteintech Group, Inc. (Chicago, IL, USA). The bicinchoninic acid protein assay kit was purchased from Novagen Inc. (Madison, WI, USA). polyvinylidene difluoride membranes were acquired from Millipore (Billerica, MA, USA). Image-Pro Plus 6.0 was purchased from Media Cybernetics (Rockville, MD, USA). Sodium dodecyl sulfate (SDS) gels for electrophoresis were purchased from ZSGB-BIO Co. Ltd. (Beijing, China). The Electrophoresis Gel Imaging Analysis system was obtained from DNR Bio-Imaging Systems Ltd. (Jerusalem, Israel). ImageJ 1.36 software was purchased from National Institutes of Health (Bethesda, MD, USA). GraphPad PRISM 6.0 software was obtained from GraphPad Software, Inc. (La Jolla, CA, USA). In total, 40 female Sprague-Dawley (SD) rats (6-8 weeks, 180-200 g) and 10 guinea pigs (4-5 weeks, 250-350 g) were obtained from the Experimental Animal Center of China Medical University (Shenyang, China). All the animals were kept under pathogen-free conditions in the Experimental Animal Center of China Medical University.

*EAE induction*. With the approval of the Bioethics Committee of China Medical University, the EAE model was established by following standard universally accepted procedures (18). In brief, guinea pig spinal cord homogenate was mixed with same amount of CFA, which contained 5 mg/ml *Mycobacterium tuberculosis* H37Ra. Each rat received a subcutaneous injection into the back and the hind footpads of 0.5 ml mixture to induce EAE. The day of immunization was regarded as Day 0 postimmunization (p.i.).

*TSIIA treatment and EAE assessment*. Forty rats were separated at random into four groups. Phosphate-buffered saline (PBS) (5 ml/kg) with dimethyl sulfoxide (DMSO) (5%) and Tween-80 (5%) was used as a drug solvent. Ten non-EAE rats that administered solvent intraperitoneally (i.p.) every day beginning from day 0 p.i. served as the naive group. Ten EAE rats administered i.p. injection of equal volume of solvent every day served as the vehicle group. In the last two groups, EAE was induced and rats were administered two different TSIIA concentrations i.p. TSIIA was dissolved in solvent at low (25 mg/kg; TSIIA-L group) and high (50 mg/kg; TSIIA-H group) concentrations, respectively. From day 0 p.i. the body weight of all rats was measured daily and clinical signs were also evaluated by two independent observers using the scale shown in Table I (19).

Table I. Clinical signs scales.

| Clinical score | Clinical sign |
|---|---|
| 0 | No clinical score |
| 1 | Loss of tail tone |
| 2 | Hindlimb weakness |
| 3 | Hindlimb paralysis |
| 4 | Forelimb paralysis |
| 5 | Moribund or death |

*Histopathological assessment*. On day 18 p.i., all the rats were sacrificed by transcardial perfusion of PBS (pH 7.4) through the left ventricle under anesthesia with injection of 10% chloral hydrate (3 ml/kg; Sinopharm Chemical Reagent Co., Ltd., Shanghai, China) into the abdominal cavity, and spinal cord and brain samples were obtained. Lumbar enlargement of the spinal cord and right-hand side of the brain were paraformaldehyde-fixed and paraffin-embedded. Subsequently, 3-$\mu$m slices of brain were sectioned and stained with hematoxylin-eosin (H&E) to evaluate inflammatory infiltration. In addition, 3-$\mu$m slices of spinal cord were sectioned and stained with LFB to evaluate demyelination. Histopathological assessment was performed in a blinded according to Table II (19).

*Immunohistochemical analysis of CD4, CD8, Mac-1, IL-17 and IL-23*. Slices (3 $\mu$m) of brain and spinal cord were used for immunohistochemical staining. After deparaffinization with xylene and washing with PBS, sections of spinal cords were incubated with rabbit antibodies specific for CD4 (diluted 1:200), CD8 (diluted 1:200), Mac-1 (diluted 1:200), IL-17 (diluted 1:200) and IL-23 (diluted 1:200). Biotin-labeled anti-rabbit IgG was used as a secondary antibody for the detection of primary antibodies. Color was developed with DAB. CD4-, CD8- and Mac-1-positive cells were counted under 400-fold magnification in the ventricornu of spinal cord sections. Expression of IL-23 and IL-17 was assessed based on the integral optical density (IOD) of positive cells under 200-fold magnification in a restricted area of brain sections. Five fields in the restricted area were randomly selected for calculations. All measurements and data analysis were performed independently by two pathologists in a blinded manner. Morphometric analysis was conducted using Image-Pro Plus 6.0.

*Western blot analysis*. Brain and spinal cord from each group was respectively homogenized in lysis buffer with protease

Table II. Histopathological assessment.

| Score | Inflammation | Demyelination |
|---|---|---|
| 0 | No inflammatory cells | None |
| 1 | A few scattered inflammatory cells | Rare foci |
| 2 | Organization of inflammatory infiltrates around blood vessels | A few areas of demyelination |
| 3 | Extensive perivascular cuffing with extension into adjacent parenchyma or parenchyma | Large (confluent) areas of demyelination |

inhibitors and RIPA for protein extraction. Tissue homogenate was centrifuged at 12,000 x g for 10 min at 4˚C to obtain the supernatants. The BCA protein assay kit was used to measure protein concentrations. Protein samples (30 $\mu$g/well) were subjected to electrophoresis on 10% SDS-PAGE gel and electrotransferred onto a PVDF membrane. After blocking with 5% non-fat dry milk in Tris-buffered saline with 0.05% Tween-20 (TBST) for 2 h at normal temperature, the membranes were separately incubated with rabbit anti-CD4 (diluted 1:500), rabbit anti-CD8 (diluted 1:500), rabbit anti-Mac-1 (diluted 1:300), rabbit anti-IL-17 (diluted 1:500), rabbit anti-IL-23 (diluted 1:500) and mouse anti-β-actin (diluted 1:1,000) overnight at 4˚C. The following day, membranes were washed three times with TBST (5 min/wash), then were incubated with peroxidase-conjugated goat anti-rabbit secondary or goat anti-mouse secondary (diluted 1:2,000) antibody for 2 h. Following incubation, the membranes were washed three times with TBST (5 min/wash). Bands were treated with Luminol reagent for 1 min and visualized using the Electrophoresis Gel Imaging Analysis system. Band density was calculated via Image J 1.36 software. Protein bands were compared with that of β-actin to determine the relative expression level of target protein.

*ELISA analysis of IL-17 and IL-23*. On day 18 p.i., all the rats were sacrificed by transcardial perfusion of PBS (pH 7.4) through the left ventricle under anesthesia with injection of 10% chloral hydrate (3 ml/kg) into the abdominal cavity, and blood was collected via retro-orbital bleeding to collect the serum. IL-17 and IL-23 concentrations were detected using ELISA according to the specifications strictly.

*Statistical analysis*. The results are presented as the mean ± standard deviation. GraphPad PRISM 6.0 software (GraphPad Software, Inc., La Jolla, CA, USA) was utilized to conduct all statistical analyses. Multiple comparisons were performed by Kruskal-Wallis test or one-way analysis of variance, followed by the least significant differences test, as appropriate. P<0.05 was considered to indicate a statistically significant difference.

## Results

*TSIIA treatment relieves clinical signs*. Clinical signs of EAE development in rats from the vehicle group began to appear on day 9 p.i., including loss of appetite, reduced physical activity, and tail and limb paralysis. However, EAE onset in TSIIA-treated rats occurred on day 11 p.i. (TSIIA-H) and 10 p.i. (TSIIA-L). Compared with the vehicle group, the two TSIIA-treated groups received significantly lower clinical scores (P<0.01). Significant differences were also observed between the treated groups, which were dose-dependent (P<0.01; Fig. 1A). Furthermore, the body weights of untreated EAE rats were significantly decreased, compared with the naive and TSIIA-treated rats (all P<0.01) while those of TSIIA-treated groups were only marginally reduced, with the smallest recorded weight loss in the TSIIA-H group. Significant differences in body weight were observed between the two treatment groups (P<0.01; Fig. 1B).

*TSIIA treatment improves CNS histopathology*. Since inflammatory cell invasion and CNS demyelination are the key characteristics of EAE, the impact of TSIIA on these parameters was verified. Consistent with clinical scores, rats in the vehicle group exhibited typical inflammatory cell infiltration in the brain, as determined via H&E staining. This cell infiltration was dose dependently attenuated following TSIIA treatment (Fig. 2A). Similarly, LFB staining revealed large areas of demyelination in the spinal cord of rats from the vehicle group, which were significantly decreased in the treated groups (both P<0.01; Fig. 2B). These results clearly indicate a beneficial effect of TSIIA in reducing inflammatory cell infiltration and demyelination, which provide the basement of mitigated clinical signs following TSIIA treatment.

*TSIIA treatment suppresses the expression of CD4, CD8 and Mac-1*. To identify the types of infiltrating cells in the CNS of EAE rats, immunohistochemistry was performed. Inflammatory exudates included a mixture of cell types, including $CD4^+$ T cells, $CD8^+$ T cells, microglia and macrophages (Fig. 3A-L). Compared with the vehicle group, TSIIA administration at the two doses induced a significant decrease in the quantity of $CD4^+$ T cells (P<0.01), $CD8^+$ T cells (P<0.01), macrophages and microglia (P<0.01) (Fig. 3M-O). The results were confirmed by quantification of the western blots and were consistent with the results of immunostaining (P<0.05; Fig. 4A, B and C).

*TSIIA treatment suppresses the levels of IL-17 and IL-23 in the brain*. Expression of the inflammatory cytokines, IL-17 and IL-23, is usually increased in the CNS in EAE. To assess whether TSIIA exerts anti-inflammatory activity in EAE *in vivo*, its effects on IL-23 and IL-17 levels in the brain were determined using immunohistochemistry. Compared with the naive group, expression of IL-17 and IL-23 in the vehicle groups was significantly increased (P<0.01). Compared with

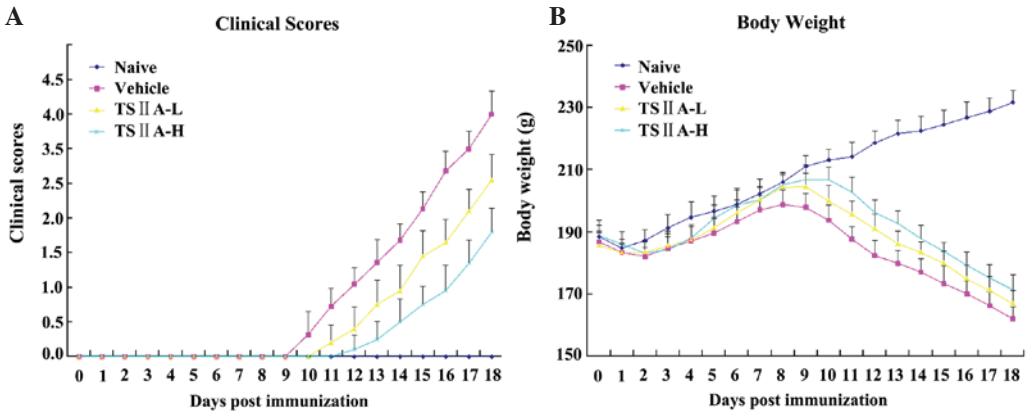


Figure 1. Clinical scores and body weight curves of rats in each group. (A) Clinical score curves of rats in each group 0-18 days post-immunization. Compared with the naive group, the clinical score in the vehicle group was significantly increased (P<0.01). Compared with the vehicle group, clinical scores in the TSIIA-treated groups were reduced significantly (both P<0.01), and there was a significant difference between the two treated groups (P<0.01). (B) Body weight curves of rats in each group. Significant weight loss was observed in the vehicle group compared with the naïve group (P<0.01), while the two TSIIA-treated groups exhibited significantly increased body weights compared with the vehicle group (P<0.01), and there was a significant difference between the TSIIA-L and TSIIA-H groups (P<0.01). Values are presented as the mean ± standard deviation (n=10 per group). TSIIA, Tanshinone IIA; TSIIA-L, TSIIA low dose; TSIIA-H, TSIIA high dose.

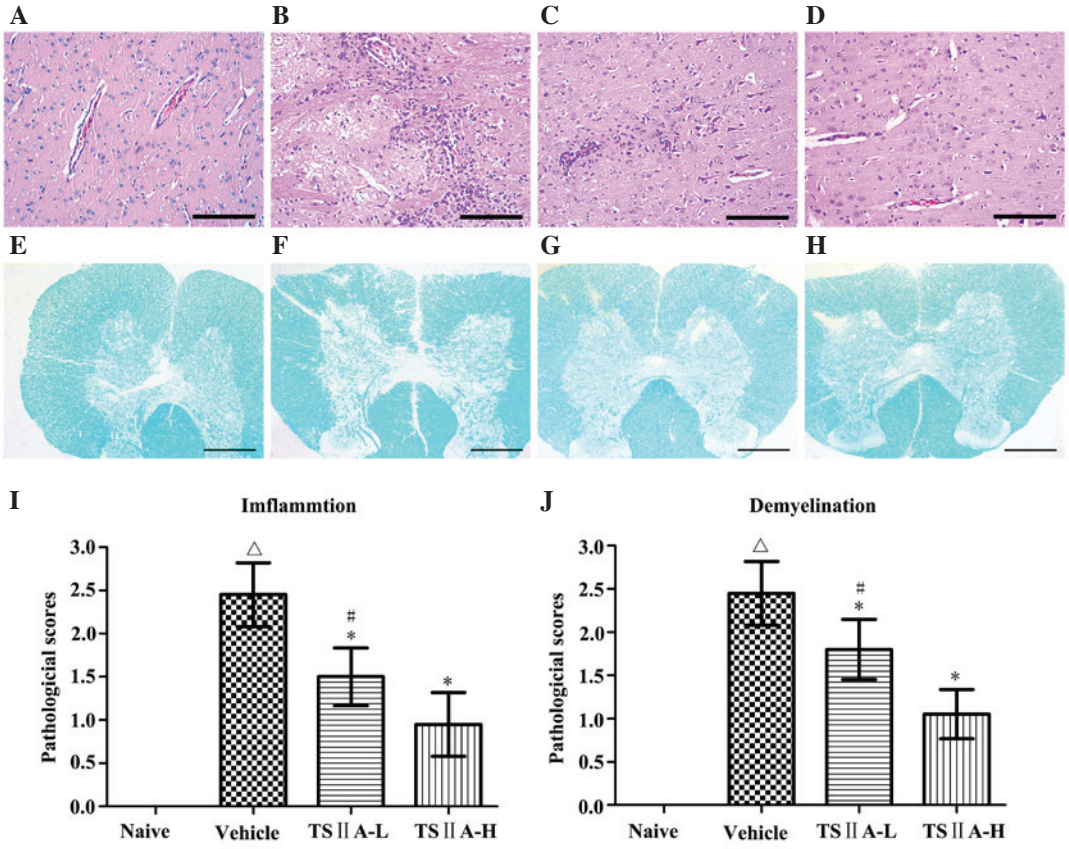


Figure 2. Histological analysis of inflammation and demyelination. (A-D) H&E staining. Magnification, x200; (E-H) LFB staining. Magnification, x5; (A and E) naive group; (B and F) vehicle group; (C and G) TSIIA-L group; (D and H) TSIIA-H group. (I) Quantification of inflammatory cell infiltration (H&E staining, A-D), (J) demyelination quantification (LFB staining, E-H). Values are presented as the mean ± standard deviation (n=10 per group). $^{\Delta}$P<0.01, compared with the naive group; $^{*}$P<0.01, compared with the vehicle group; $^{\#}$P<0.01, compared with the TSIIA-H group. TSIIA, Tanshinone IIA; LFB, Luxol Fast Blue; H&E, hematoxylin and eosin.

the vehicle group, TSIIA treatment significantly induced a reduction in IL-17 and IL-23 expression (P<0.01). However, there were no significant differences between the two treatment groups (P>0.05; Fig. 5). The effects of TSIIA on these indicators were further confirmed by quantitative western blot analysis (P<0.01), and significant differences were identified between the TSIIA-L and TSIIA-H groups in IL-17 (P<0.01) and IL-23 (P<0.05) expression (Fig. 4 A, E and F).

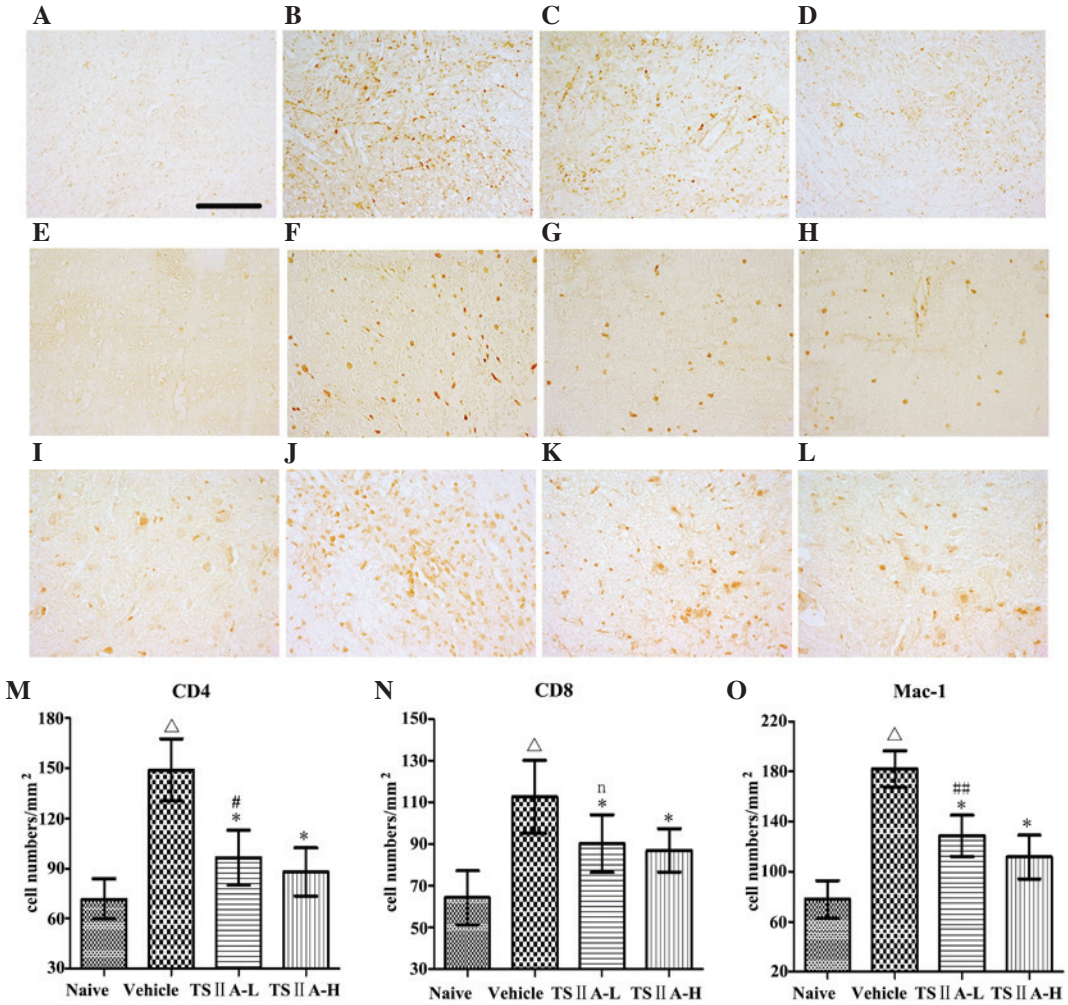


Figure 3. Immunohistochemistry of CD4, CD8 and Mac-1. (A-D) CD4; (E-H) CD8; (I-L) Mac-1; Magnification, x400. (A, E and I) naive group; (B, F and J) vehicle group; (C, G and K) TSIIA-L group; and (D, H and L) TSIIA-H group. (M-O) Quantitative analysis of the above immune cells. Values are presented as the mean ± standard deviation (n=10 per group). $^{\Delta}$P<0.01, compared with the naive group; $^{*}$P<0.01, compared with the vehicle group; $^{\#}$P<0.01, $^{\#\#}$P<0.05 or n (not significant) compared with the TSIIA-H group. TSIIA, Tanshinone IIA; TSIIA-L, TSIIA low dose; TSIIA-H, TSIIA high dose.

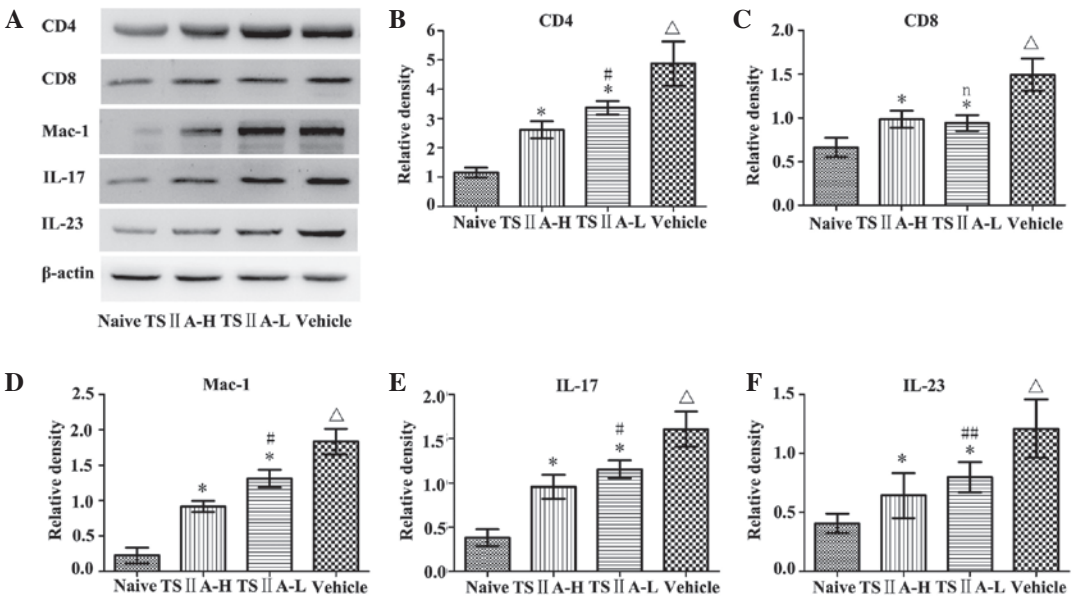


Figure 4. (A) Determination of CD4, CD8, Mac-1, IL-17 and IL-23 protein expression via western blot analysis. Quantitative analysis of (B) CD4, (C) CD8, (D) Mac-1, (E) IL-17 and (F) IL-23. Values are presented as the mean ± standard deviation (n=10 per group). $^{\Delta}$P<0.01, compared with the naive group; $^{*}$P<0.01, compared with the vehicle group; $^{\#}$P<0.01, $^{\#\#}$P<0.05 or n (not significant) compared with the TSIIA-H group. TSIIA, Tanshinone IIA; IL, interleukin; TSIIA-L, TSIIA low dose; TSIIA-H, TSIIA high dose.

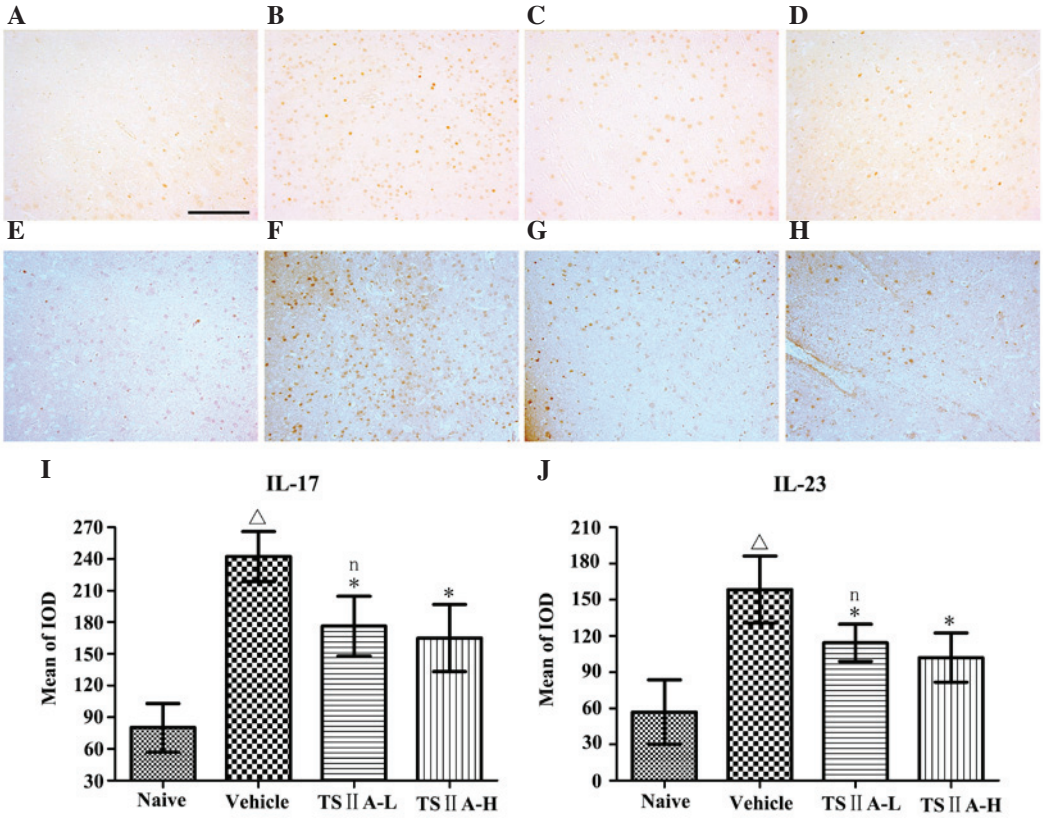


Figure 5. Immunohistochemistry of IL-17 and IL-23. (A-D) IL-17; (E-H) IL-23; Magnification, x200. (A and E) Naive group; (B and F) vehicle group; (C and G) TSIIA-L group; and (D and H) TSIIA-H group. Quantitative analysis of (I) IL-17 and (J) IL-23 was conducted. Values are presented as the mean ± standard deviation (n=10 per group). $^{\Delta}$P<0.01, compared with the naive group; $^{*}$P<0.01, compared with the vehicle group or n (not significant) between the TSIIA-L and TSIIA-H groups. IOD, integral optical density; IL, interleukin; TSIIA, Tanshinone IIA; TSIIA-L, TSIIA low dose; TSIIA-H, TSIIA high dose.

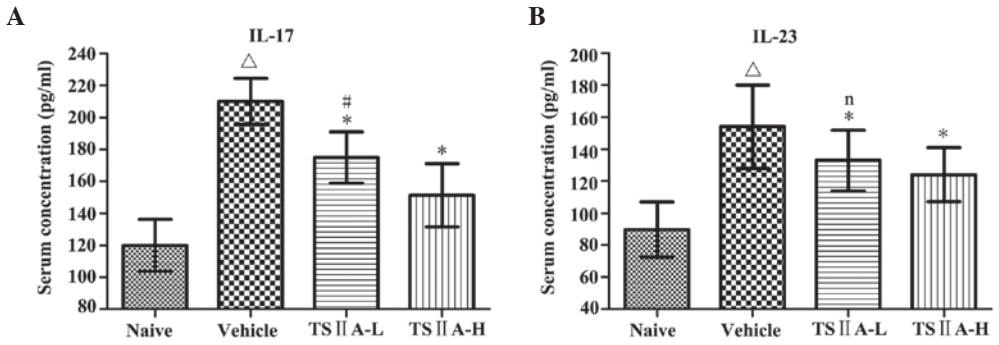


Figure 6. Measurement of serum production of (A) IL-17 and (B) IL-23 via enzyme-linked immunosorbent assay. $^{\Delta}$P<0.01, compared with the naive group; $^{*}$P<0.01, compared with the vehicle group; $^{\#}$P<0.01 or or n (not significant) compared with the TSIIA-H group. IL, interleukin; TSIIA, Tanshinone IIA; TSIIA-L, TSIIA low dose; TSIIA-H, TSIIA high dose.

*TSIIA treatment reduces the expression of IL-17 and IL-23 in the serum*. The serum contents of IL-17 and IL-23 are usually upregulated and closely associated with the development of EAE. The highest concentrations of serum IL-17 and IL-23 among all groups were found in vehicle-treated rats, which decreased significantly in the two TSIIA-treated groups (P<0.01). The serum level of IL-17 in the TSIIA-H group was lower than that in the TSIIA-L group (P<0.01). However, no significant difference was identified in the serum concentrations of IL-23 between the two TSIIA-treated groups (Fig. 6).

## Discussion

TSIIA has been shown to alleviate several CNS disorders in animal models, possibly through its anti-inflammatory and neuroprotective properties. However, the effects of TSIIA on EAE have not been determined to date. In the current study, an experimental model was established to determine the effects of TSIIA on EAE and its mechanisms of action.

In MS and EAE, $CD4^{+}$ T cells, $CD8^{+}$ T cells, macrophages and resident microglia orchestrate a series of inflammatory reactions in the CNS of humans and animals, resulting in

persistent disability. $CD4^+$ cells are undoubtedly the pivotal pathogenic cells in MS and EAE that facilitate inflammatory reactions and subsequent neurodegeneration. These cells induce neuronal death under pathological conditions through a variety of mechanisms, such as triggering antigen-independent calcium oscillations and TRAIL-mediated injury in neurons (20,21). A number of therapeutic options that reduce the T cell- and particularly, $CD4^+$ cell-mediated damage of neurons are extensively applied in the clinic. For example, natalizumab, an effective drug for MS, decreases the number of $CD4^+$ cells in the brain and inhibits peripheral lymphocyte migration into the CNS (22). $CD8^+$ T cells are also crucial in CNS autoimmunity. These cells are abundant in active demyelinating lesions in MS, and induce inflammation and demyelination in EAE (23). Furthermore, there is a positive correlation between the degree of axonal injury and the quantity of $CD8^+$ T cells as well as macrophages/microglia in the brain tissue from patients with MS, suggesting their important effects on axon loss (24). Cytotoxic $CD8^+$ T cells secrete various pro-inflammatory cytokines, including perforin (25) and granzymes (26), which trigger autoimmune injury mediated by cells in the CNS. Sodium tanshinone IIA sulfonate, a water-soluble derivative of TSIIA, has been shown to markedly suppress the proliferation of spleen T lymphocytes and reduce the $CD4^+$ and $CD8^+$ T cell percentage in peripheral blood in a rat skin transplantation model (27). Additionally, TSIIA inhibits the maturation of dendritic cells and suppresses the expression of pro-inflammatory cytokines, weakening their capacity to stimulate T-cell proliferation (28). Data from the current study showed that TSIIA downregulates the increase in $CD4^+$ and $CD8^+$ T cells in the CNS and relieves clinical symptoms.

Macrophages in the CNS are derived from peripheral monocytes, and microglia are resident macrophages. Once activated, microglia and macrophages cause mitochondrial dysfunction through induction of reactive oxygen and nitrogen species, which contribute to axon injury and subsequent neuronal cell death (29). Activated microglia and macrophages produce pro-inflammatory cytokines and enhance sensitization of axons to glutamate, with subsequent initiation of an indirect immunological attack on oligodendrocytes and neurons (30,31). TSIIA reduces the release of LPS-induced pro-inflammatory cytokines, such as IL-1, IL-6 and tumor necrosis factor (TNF)-α, from macrophages during inflammation (32-34). Microglial activation, a hallmark of CNS pathology in MS and other neurodegenerative diseases, triggers cytotoxic effects and drives neuronal damage, which can be suppressed by TSIIA in experimental models of SNL-induced neuropathic pain (35) and Parkinson's disease (13). Macrophage depletion (36) and microglial paralysis (37) markedly alleviate disease progression. Consistently, compared with wild-type mice, Mac-1-deficient mice displayed attenuated EAE with lower levels of gliosis, axonal degeneration and demyelination (38). To the best of our knowledge, no studies regarding the impact of TSIIA on microglia/macrophages in CNS of EAE are have been conducted. The results from this study showed that following TSIIA treatment, microglia/macrophage numbers are decreased following decreased demyelination and inflammatory cell infiltration in the CNS of EAE rats.

The IL-17/IL-23 pathway is associated with the pathogenesis of autoimmune disorders, including MS, psoriasis and inflammatory bowel disease (39-41). IL-23-deficient mice are unable to induce EAE (42). IL-23 is reported to promote polarization, development and expansion of pathogenic T cells; thus, it is essential for EAE induction. (43-45). As a lineage of major pathogenic T cells, Th17 cells not only autosynthesize but also promote other types of cells to generate pro-inflammatory cytokines (46). Furthermore, Th17 cells transmigrate efficiently across the blood brain barrier, damage neurons and contribute to CNS inflammation through $CD4^+$ lymphocyte accumulation (47). Targeting IL-23-p19 with neutralizing antibodies has been shown to reduce the IL-17 level in the CNS and serum, which was also shown to prevent EAE relapse during disease remission (48). Serum IL-17 levels are positively correlated with disease severity (49) and EAE is inhibited in $IL\text{-}17^{-/-}$ mice whose $CD4^+$ T cells are incapable of inducing EAE efficiently, compared with wild-type T cells (50). IL-17 also stimulates microglia (51) and astrocytes (52) to secrete inflammatory cytokines and chemokines, resulting in recruitment of neutrophils (53). In collaboration with TNF-α, IL-17 promotes oxidative stress-induced apoptosis of oligodendrocytes, causing axonal loss and subsequent neurological deficits (54,55). In an earlier phase II clinical trial, following treatment with secukinumab, an antibody that neutralizes IL-17, MS patients displayed fewer new CNS lesions observed using magnetic resonance imaging, and lower annualized recurrence rates, compared with placebo-treated patients (56). Therefore, blockage of the IL-23/IL-17 pathway in the clinical treatment of MS has recently received considerable research attention, in view of accumulating data highlighting its vital role in MS/EAE. TSIIA has been shown to inhibit IL-17-induced vascular remodeling in systemic sclerosis patients (17). However, no research to date has investigated the impact of TSIIA on IL-17 and IL-23 levels in EAE/MS. To the best of our knowledge, this is the first study to demonstrate a significant decrease in serum and brain expression of IL-17 and IL-23 in EAE following TSIIA treatment.

In conclusion, this study provides preliminary evidence supporting the use of TSIIA as a potential novel therapeutic option for MS. However, rats in this study were only treated acutely, and the feasibility and safety of TSIIA require validation in the clinic.

## Acknowledgements

This study was supported by the Liaoning Province Science and Technology Project-Animal Scientific Research and Clinical Application for Major Disease of Liaoning Province (grant no. 2012225021), Program of Basic and Clinical Research Platform of China Medical University (grant no. CMU-201406) and from Technology Projects of Liaoning Province (grant no. 2009225010-2) to Dr Juan Feng.

## References

1. Rangachari M and Kuchroo VK: Using EAE to better understand principles of immune function and autoimmune pathology. J Autoimmun 45: 31-39, 2013.
2. Leuenberger T, Paterka M, Reuter E, Herz J, Niesner RA, Radbruch H, Bopp T, Zipp F and Siffrin V: The role of CD8 (+) T cells and their local interaction with CD4 (+) T cells in myelin oligodendrocyte glycoprotein (35-55)-induced experimental autoimmune encephalomyelitis. J Immunol 191: 4960-4968, 2013.

3. Cabarrocas J, Bauer J, Piaggio E, Liblau R and Lassmann H: Effective and selective immune surveillance of the brain by MHC class I-restricted cytotoxic T lymphocytes. Eur J Immunol 33: 1174-1182, 2003.
4. Fischer HG and Reichmann G: Brain dendritic cells and macrophages/microglia in central nervous system inflammation. J Immunol 166: 2717-2726, 2001.
5. Li Y, Chu N, Hu A, Gran B, Rostami A and Zhang GX: Increased IL-23p19 expression in multiple sclerosis lesions and its induction in microglia. Brain 130: 490-501, 2007.
6. Langrish CL, Chen Y, Blumenschein WM, Mattson J, Basham B, Sedgwick JD, McClanahan T, Kastelein RA and Cua DJ: IL-23 drives a pathogenic T cell population that induces autoimmune inflammation. J Exp Med 201: 233-240, 2005.
7. Luchtman DW, Ellwardt E, Larochelle C and Zipp F: IL-17 and related cytokines involved in the pathology and immunotherapy of multiple sclerosis: Current and future developments. Cytokine Growth Factor Rev 25: 403-413, 2014.
8. McFarland HF and Martin R: Multiple sclerosis: A complicated picture of autoimmunity. Nat Immunol 8: 913-919, 2007.
9. Castro-Borrero W, Graves D, Frohman TC, Flores AB, Hardeman P, Logan D, Orchard M, Greenberg B and Frohman EM: Current and emerging therapies in multiple sclerosis: A systematic review. Ther Adv Neurol Disord 5: 205-220, 2012.
10. Wu B, Liu M and Zhang S: Cochrane systematic review: danshen agents for acute ischaemic stroke. Chinese Journal of Evidence-Based Medicine 2: 101-105, 2005.
11. Cheng TO: Cardiovascular effects of Danshen. Int J Cardiol 121: 9-22, 2007.
12. Xu S and Liu P: Tanshinone II-A: New perspectives for old remedies. Expert Opin Ther Pat 23: 149-153, 2013.
13. Ren B, Zhang YX, Zhou HX, Sun FW, Zhang ZF, Wei Z, Zhang CY and Si DW: Tanshinone IIA prevents the loss of nigrostriatal dopaminergic neurons by inhibiting NADPH oxidase and iNOS in the MPTP model of Parkinson's disease. J Neurol Sci 348: 142-152, 2015.
14. Jiang P, Li C, Xiang Z and Jiao B: Tanshinone IIA reduces the risk of Alzheimer's disease by inhibiting iNOS, MMP-2 and NF-κBp65 transcription and translation in the temporal lobes of rat models of Alzheimer's disease. Mol Med Rep 10: 689-694, 2014.
15. Zhang K, Wang J, Jiang H, Xu X, Wang S, Zhang C, Li Z, Gong X and Lu W: Tanshinone IIA inhibits lipopolysaccharide-induced MUC1 overexpression in alveolar epithelial cells. Am J Physiol Cell Physiol 306: C59-C65, 2014.
16. Zhu W, Lu Q, Chen HW, Feng J, Wan L and Zhou DX: Protective effect of sodium tanshinone II A sulfonate on injury of small intestine in rats with sepsis and its mechanism. Chin J Integr Med 18: 496-501, 2012.
17. Liu M, Yang J and Li M: Tanshinone IIA attenuates interleukin-17A-induced systemic sclerosis patient-derived dermal vascular smooth muscle cell activation via inhibition of the extracellular signal-regulated kinase signaling pathway. Clinics (Sao Paulo) 70: 250-256, 2015.
18. Mao YS, Lu CZ, Wang X and Xiao BG: Induction of experimental autoimmune encephalomyelitis in Lewis rats by a viral peptide with limited homology to myelin basic protein. Exp Neurol 206: 231-239, 2007.
19. Jokubaitis VG, Gresle MM, Kemper DA, Doherty W, Perreau VM, Cipriani TL, Jonas A, Shaw G, Kuhlmann T, Kilpatrick TJ and Butzkueven H: Endogenously regulated Dab2 worsens inflammatory injury in experimental autoimmune encephalomyelitis. Acta Neuropathol Commun 1: 32, 2013.
20. Nitsch R, Pohl EE, Smorodchenko A, Infante-Duarte C, Aktas O and Zipp F: Direct impact of T cells on neurons revealed by two-photon microscopy in living brain tissue. J Neurosci 24: 2458-2464, 2004.
21. Aktas O, Smorodchenko A, Brocke S, Infante-Duarte C, Schulze Topphoff U, Vogt J, Prozorovski T, Meier S, Osmanova V, Pohl E, *et al*: Neuronal damage in autoimmune neuroinflammation mediated by the death ligand TRAIL. Neuron 46: 421-432, 2005.
22. del Pilar Martin M, Cravens PD, Winger R, Frohman EM, Racke MK, Eagar TN, Zamvil SS, Weber MS, Hemmer B, Karandikar NJ, *et al*: Decrease in the numbers of dendritic cells and CD4+ T cells in cerebral perivascular spaces due to natalizumab. Arch Neurol 65: 1596-1603, 2008.
23. Babbe H, Roers A, Waisman A, Lassmann H, Goebels N, Hohlfeld R, Friese M, Schröder R, Deckert M, Schmidt S, *et al*: Clonal expansions of CD8 (+) T cells dominate the T cell infiltrate in active multiple sclerosis lesions as shown by micromanipulation and single cell polymerase chain reaction. J Exp Med 192: 393-404, 2000.
24. Kuhlmann T, Lingfeld G, Bitsch A, Schuchardt J and Brück W: Acute axonal damage in multiple sclerosis is most extensive in early disease stages and decreases over time. Brain 125: 2202-2212, 2002.
25. Meuth SG, Herrmann AM, Simon OJ, Siffrin V, Melzer N, Bittner S, Meuth P, Langer HF, Hallermann S, Boldakowa N, *et al*: Cytotoxic CD8+ T cell-neuron interactions: Perforin-dependent electrical silencing precedes but is not causally linked to neuronal cell death. J Neurosci 29: 15397-15409, 2009.
26. Zang YC, Li S, Rivera VM, Hong J, Robinson RR, Breitbach WT, Killian J and Zhang JZ: Increased CD8+ cytotoxic T cell responses to myelin basic protein in multiple sclerosis. J Immunol 172: 5120-5127, 2004.
27. Yu Q, Chen H, Sheng L, Liang Y and Li Q: Sodium tanshinone IIA sulfonate prolongs the survival of skin allografts by inhibiting inflammatory cell infiltration and T cell proliferation. Int Immunopharmacol 22: 277-284, 2014.
28. Li HZ, Lu YH, Huang GS, Chen Q, Fu Q and Li ZL: Tanshinone II A inhibits dendritic cell-mediated adaptive immunity: Potential role in anti-atherosclerotic activity. Chin J Integr Med 20: 764-769, 2014.
29. Nikić I, Merkler D, Sorbara C, Brinkoetter M, Kreutzfeldt M, Bareyre FM, Brück W, Bishop D, Misgeld T and Kerschensteiner M: A reversible form of axon damage in experimental autoimmune encephalomyelitis and multiple sclerosis. Nat Med 17: 495-499, 2011.
30. Pitt D, Werner P and Raine CS: Glutamate excitotoxicity in a model of multiple sclerosis. Nat Med 6: 67-70, 2000.
31. Jack C, Ruffini F, Bar-Or A and Antel JP: Microglia and multiple sclerosis. J Neurosci Res 81: 363-373, 2005.
32. Chen TH, Hsu YT, Chen CH, Kao SH and Lee HM: Tanshinone IIA from Salvia miltiorrhiza induces heme oxygenase-1 expression and inhibits lipopolysaccharide-induced nitric oxide expression in RAW 264.7 cells. Mitochondrion 7: 101-105, 2007.
33. Choi HS, Cho DI, Choi HK, Im SY, Ryu SY and Kim KM: Molecular mechanisms of inhibitory activities of tanshinones on lipopolysaccharide-induced nitric oxide generation in RAW 264.7 cells. Arch Pharm Res 27: 1233-1237, 2004.
34. Fan GW, Gao XM, Wang H, Zhu Y, Zhang J, Hu LM, Su YF, Kang LY and Zhang BL: The anti-inflammatory activities of Tanshinone IIA, an active component of TCM, are mediated by estrogen receptor activation and inhibition of iNOS. J Steroid Biochem Mol Biol 113: 275-280, 2009.
35. Cao FL, Xu M, Wang Y, Gong KR and Zhang JT: Tanshinone IIA attenuates neuropathic pain via inhibiting glial activation and immune response. Pharmacol Biochem Behav 128: 1-7, 2015.
36. Huitinga I, van Rooijen N, de Groot CJ, Uitdehaag BM and Dijkstra CD: Suppression of experimental allergic encephalomyelitis in Lewis rats after elimination of macrophages. J Exp Med 172: 1025-1033, 1990.
37. Heppner FL, Greter M, Marino D, Falsig J, Raivich G, Hövelmeyer N, Waisman A, Rülicke T, Prinz M, Priller J, *et al*: Experimental autoimmune encephalomyelitis repressed by microglial paralysis. Nat Med 11: 146-152, 2005.
38. Bullard DC, Hu X, Schoeb TR, Axtell RC, Raman C and Barnum SR: Critical requirement of CD11b (Mac-1) on T cells and accessory cells for development of experimental autoimmune encephalomyelitis. J Immunol 175: 6327-6333, 2005.
39. Qin S, Wen J, Bai XC, Chen TY, Zheng RC, Zhou GB, Ma J, Feng JY, Zhong BL and Li YM: Endogenous n-3 polyunsaturated fatty acids protect against imiquimod-induced psoriasis-like inflammation via the IL-17/IL-23 axis. Mol Med Rep 9: 2097-2104, 2014.
40. Ghadimi D, Helwig U, Schrezenmeir J, Heller KJ and de Vrese M: Epigenetic imprinting by commensal probiotics inhibits the IL-23/IL-17 axis in an in vitro model of the intestinal mucosal immune system. J Leukoc Biol 92: 895-911, 2012.
41. Gaffen SL, Jain R, Garg AV and Cua DJ: The IL-23-IL-17 immune axis: From mechanisms to therapeutic testing. Nat Rev Immunol 14: 585-600, 2014.
42. Cua DJ, Sherlock J, Chen Y, Murphy CA, Joyce B, Seymour B, Lucian L, To W, Kwan S, Churakova T, *et al*: Interleukin-23 rather than interleukin-12 is the critical cytokine for autoimmune inflammation of the brain. Nature 421: 744-748, 2003.
43. McGeachy MJ, Chen Y, Tato CM, Laurence A, Joyce-Shaikh B, Blumenschein WM, McClanahan TK, O'Shea JJ and Cua DJ: The interleukin 23 receptor is essential for the terminal differentiation of interleukin 17-producing effector T helper cells in vivo. Nat Immunol 10: 314-324, 2009.
44. Gyuelveszi G, Haak S and Becher B: IL-23-driven encephalo-tropism and Th17 polarization during CNS-inflammation in vivo. Eur J Immunol 39: 1864-1869, 2009.

45. Ghoreschi K, Laurence A, Yang XP, Tato CM, McGeachy MJ, Konkel JE, Ramos HL, Wei L, Davidson TS, Bouladoux N, *et al*: Generation of pathogenic T (H) 17 cells in the absence of TGF-β signalling. Nature 467: 967-971, 2010.
46. Goverman J: Autoimmune T cell responses in the central nervous system. Nat Rev Immunol 9: 393-407, 2009.
47. Kebir H, Kreymborg K, Ifergan I, Dodelet-Devillers A, Cayrol R, Bernard M, Giuliani F, Arbour N, Becher B and Prat A: Human TH17 lymphocytes promote blood-brain barrier disruption and central nervous system inflammation. Nat Med 13: 1173-1175, 2007.
48. Chen Y, Langrish CL, McKenzie B, Joyce-Shaikh B, Stumhofer JS, McClanahan T, Blumenschein W, Churakovsa T, Low J, Presta L, *et al*: Anti-IL-23 therapy inhibits multiple inflammatory pathways and ameliorates autoimmune encephalomyelitis. J Clin Invest 116: 1317-1326, 2006.
49. Tzartos JS, Friese MA, Craner MJ, Palace J, Newcombe J, Esiri MM and Fugger L: Interleukin-17 production in central nervous system-infiltrating T cells and glial cells is associated with active disease in multiple sclerosis. Am J Pathol 172: 146-155, 2008.
50. Komiyama Y, Nakae S, Matsuki T, Nambu A, Ishigame H, Kakuta S, Sudo K and Iwakura Y: IL-17 plays an important role in the development of experimental autoimmune encephalomyelitis. J Immunol 177: 566-573, 2006.
51. Kawanokuchi J, Shimizu K, Nitta A, Yamada K, Mizuno T, Takeuchi H and Suzumura A: Production and functions of IL-17 in microglia. J Neuroimmunol 194: 54-61, 2008.
52. Trajkovic V, Stosic-Grujicic S, Samardzic T, Markovic M, Miljkovic D, Ramic Z and Mostarica Stojkovic M: Interleukin-17 stimulates inducible nitric oxide synthase activation in rodent astrocytes. J Neuroimmunol 119: 183-191, 2001.
53. Wojkowska DW, Szpakowski P, Ksiazek-Winiarek D, Leszczynski M and Glabinski A: Interactions between neutrophils, Th17 cells and chemokines during the initiation of experimental model of multiple sclerosis. Mediators Inflamm 2014: 590409, 2014.
54. Paintlia MK, Paintlia AS, Singh AK and Singh I: Synergistic activity of interleukin-17 and tumor necrosis factor-α enhances oxidative stress-mediated oligodendrocyte apoptosis. J Neurochem 116: 508-521, 2011.
55. Prineas JW, Barnard RO, Kwon EE, Sharer LR and Cho ES: Multiple sclerosis: Remyelination of nascent lesions. Ann Neurol 33: 137-151, 1993.
56. Miossec P and Kolls JK: Targeting IL-17and TH17 cells in chronic inflammation. Nat Rev Drug Discov 11: 763-776, 2012.